Viscoelastic Characterization of *in vivo* Human Dermis Using High-Frequency Ultrasonic Crawling Wave Elastography

ANA C. SAAVEDRA[1], (Member, IEEE), **JUNIOR ARROYO**[1], **GILMER FLORES**[1], (Member, IEEE),
FERNANDO ZVIETCOVICH[1,2], **BENJAMIN CASTANEDA**[1], (Senior Member, IEEE),
AND ROBERTO J. LAVARELLO[1], (Senior Member, IEEE)

[1]Department of Engineering, Pontificia Universidad Católica del Perú, Lima 15088, Peru
[2]Daza de Valdes Institute of Optics, Spanish National Research Council (CSIC), 28006 Madrid, Spain

Corresponding author: Roberto J. Lavarello (lavarello.rj@pucp.edu.pe)

ABSTRACT High-frequency (center frequency of 18MHz) ultrasound was combined with crawling wave elastography to characterize skin viscoelastic properties in two anatomical sites (i.e., thigh and forearm) in humans in the range of 200-400 Hz. The Voigt model was used to obtain shear elasticity and shear viscosity estimates. The forearm's mean shear elasticity and shear viscosity were 6 kPa and 5.5 Pa.s, respectively, exhibiting significantly higher values than in the thigh (3.4 kPa and 3.2 Pa.s, respectively, $p < 0.05$). These results suggest that skin viscoelastic properties can be estimated *in vivo* using high-frequency crawling wave elastography and show translation potential for future application in the clinical screening of skin disorders.

INDEX TERMS Skin characterization, elastography, crawling wave elastography, high-frequency ultrasound, shear waves, surface acoustic waves.

I. INTRODUCTION

Skin biomechanical properties depend on age, anatomical site, race, and other factors that complicate the development of a repeatable and consistent tissue biomarker for disease diagnosis and treatment monitoring [1], [2]. Therefore, the development of non-invasive methods that provide information about the skin structure and biomechanics (e.g., thickness, elasticity, viscosity, among others) is essential. For instance, it has been demonstrated that systemic sclerosis onset and progression causes the increase of Young's modulus in human skin [3]. Then, differentiating biomechanical abnormalities could help to diagnose and to treat skin diseases, as well as to evaluate the effects of cosmetic products and skin aging.

Several studies have reported the use of elastography methods for characterizing the skin elasticity, including skin suction [4], [5], the use of a twistometer [6], the measurement

of the strain-stress relationship [7], and the propagation of mechanical waves [3]. This latter technique, also called wave-based elastography, has shown great potential for the viscoelastic characterization of *in vivo* skin tissues using supersonic shear imaging (SSI) [8], shear wave elastography [3], [9], acoustic radiation force imaging (ARFI) [10], and crawling wave elastography [11]. In contrast, reports on the viscosity component of *in vivo* skin are fairly limited due to the high damping and attenuation of shear and surface acoustic waves in such tissues. A few reports can be found using external vibration and either laser vibrometer [12] or ultrasound probe [13] to measure the surface wave dispersion and attenuation.

This article aims to contribute to the viscoelastic analysis of the skin *in vivo* using crawling wave elastography based on high-frequency ultrasound, which allows better resolving skin layers with high resolution. The results in this article expand the ones in [11] by increasing the number of volunteers, analyzing two anatomical sites, and estimating viscoelastic parameters compared to estimates available in the state-of-the-art.
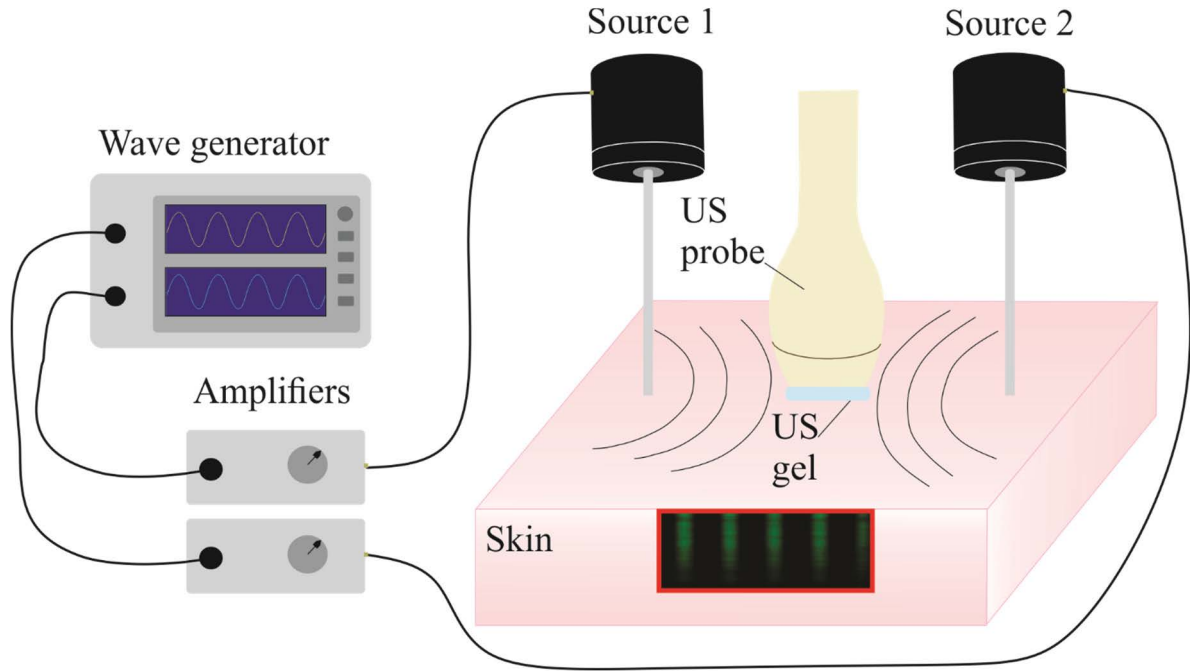
FIGURE 1. Experimental setup of high-frequency ultrasonic crawling wave elastography. The ultrasonic probe is located in between the two vibration sources (mini-shakers). A layer of ultrasound gel serves as a coupling medium between the probe and the skin tissue. Each source is excited with harmonic signals of ω and $\omega + \Delta\omega$ rad/s in order to generate the crawling wave. Excitation signals were created by a two-channel wave generator and amplified with independent power amplifiers. The red rectangle corresponds to the imaging region of interest (20 mm x 23 mm) where the green vertical stripes represent a Doppler frame capturing the motion produce by crawling wave propagation at a specific temporal instant.

II. MATERIALS AND METHODS

A. CRAWLING WAVE INTERFERENCE PATTERN

This method consists of generating a dynamic interference pattern through external vibration of two sources in opposite directions [14], as shown in Fig. 1. This model assumes that two harmonic plane waves are generated and propagated parallel to the x-axis with two different frequencies ω and $\omega + \Delta\omega$ (in this work, $\Delta\omega = 0.8\pi$ rad/s for all experiments). Under these assumptions, the squared amplitude of the interference of both mechanical waves is given by

$$|u(x,t)|^2 = 2A^2 e^{(-\alpha D)}\{cos[(2k + \Delta k)x + \Delta\omega t - (\Delta k/2)D - \Delta\varphi] + cosh(2\alpha x)\}, \quad (1)$$

where $\Delta\varphi \Delta\varphi$ is the initial phase difference between sources, A is the vibration amplitude, D is the distance separating the two sources, α is the shear wave attenuation coefficient in the medium, and kk and $(k + \Delta k)$ are the wavenumbers of both waves. The first term inside the curly braces of (1) is oscillatory and corresponds to the slow-speed wave (i.e., the crawling wave) traveling at the $C_{CrW} = \Delta\omega/(2k + \Delta k)c_{CrW} = \Delta\omega/(2k + \Delta k)$. The second term (i.e., hyperbolic cosine) refers to the attenuation of the medium, and it is slow-varying compared to the first term; then, it can be eliminated using a low-pass filter.

B. ELASTICITY ESTIMATION

Wave-based elastography leverages the relationship between mechanical wave speed and the elastic modulus of the

interrogated tissue. If the wave in question is a shear wave traveling in a homogeneous and isotropic elastic solid, then the shear wave speed (c_s) is given by [15]:

$$c_s = \sqrt{\mu}/\rho, \quad (2)$$

where μ is the shear modulus of the tissue, and ρ is its density (considered as 1020 kg/m^3 for soft tissues). Moreover, (2) can be extended to Young's modulus (E) if the incompressibility condition (i.e., Poisson's ratio $v \approx 0.5$, which is satisfied in soft tissues) is assumed, leading to $E \approx 3\mu^2$ [15].

However, skin imaging can be modeled as a problem with a semi-infinite boundary condition. Therefore, surface acoustic waves guided by the skin surface are the most dominant perturbation and, assuming the incompressibility condition of the tissue, it propagates at the speed of [16]

$$c_{sw}(\omega) \approx 0.95 \cdot c_s(\omega) \quad (3)$$

where $c_{sw}(\omega)$ is the surface wave speed.

The calculation of $c_{sw}(\omega)$ from the crawling wave interference pattern was conducted using a phase-based estimator proposed in [16]. Considering $\Delta k \ll \Delta k \ll k$k (which occurs when $\Delta\omega \ll \omega$), the spatial phase extracted from the oscillatory term of (1) becomes

$$\phi(x) = 2kx + (\Delta k/2)D - \Delta\varphi. \quad (4)$$

Then, the spatial-dependent wave number $k(x)$ can be calculated taking the spatial derivative of $\phi(x)$ as

$$k(x) = \phi'(x)/2, \quad (5)$$

where $\phi'(x) = \partial\phi(x)/\partial x$. Then, $c_{sw}(\omega)$ is given by [17]:

$$c_{sw}(\omega) = \omega/k(x) = 4\pi f/\phi'(x), \tag{6}$$

where $\omega = 2\pi f$ and f is the excitation frequency (in Hz)

C. VOIGT MODEL OF TISSUE VISCOELASTICITY

Up to this point, we were considering the tissue as an elastic solid with no viscosity. However, research has demonstrated that skin is indeed viscoelastic [18]. The Voigt model is one of the simplest rheological models for deriving viscoelastic parameters, where the frequency-dependent shear modulus is modeled as a complex number [19]:

$$\mu(\omega) = \mu_1 + i\mu_2\omega \tag{7}$$

where μ_1 [Pa] and μ_2 [Pa·s] represent the shear elasticity and the shear viscosity, respectively. Then, replacing (7) in (2) gives [19]:

$$c_s(\omega) = c_0 \left[\frac{1}{2} \cdot \frac{1}{(1 + \omega^2/\omega_0^2)} \cdot \left(\sqrt{1 + \omega^2/\omega_0^2} + 1 \right) \right]^{-1/2} \tag{8}$$

where $c_0^2 = \mu_1/\rho$ $c_0 = \sqrt{\mu_1}/\rho$, and $\omega_0 = \mu_1/\mu_2\omega_0 = \mu_1/\mu_2$. The shear wave speed becomes frequency dispersive as $\mu_2\mu_2 > 0 > 0$. Then, the viscoelastic parameters $\mu_1\mu_1$ and $\mu_2\mu_2$ can be estimated by fitting (8) to a speed dispersion plot.

D. SELECTION OF VOLUNTEERS

The Institutional Review Board of Pontificia Universidad Católica del Perú (Lima, Peru) approved this study. All volunteers signed the informed consent. A total of 18 volunteers without skin injuries or abnormalities were recruited and divided into two groups: 12 volunteers (6 males and 6 females) scanned in their thighs, and 6 volunteers (4 males and 2 females) surveyed in their forearms. The age range of all the volunteers was from 18 to 30 years old (24.5 ± 3.75 years).

The volunteers sat on the edge of a stretcher in both experiments since it was the most comfortable position. The transducer was put in contact with the skin surface through a thick layer of ultrasound gel (thickness ∼1 cm) used as a coupling acoustic medium during the imaging process. To acquire the forearm images, volunteers rested their arm on a table showing the ventral side with the probe aligned along the Langer's lines over the brachioradialis and flexor carpi radialis muscles. For imaging the thigh, the transducer was placed at the central part of the anterior thigh, aligned along the Langer's lines over the rectus femoris muscle.

E. DATA ACQUISITION AND PROCESSING

The experimental setup consisted of a commercial high-frequency ultrasound (HF-US) imaging system Vevo 2100 (Fujifilm Visualsonics Inc., Toronto, Canada) equipped with a linear-array transducer probe working at 18 MHz (model

MS250) with a pulse repetition frequency (PRF) in the range of 1 to 1.5 kHz.

After placing the ultrasound probe, two mini-shakers (type 4810, Brüel and Kjær, Nærum, Denmark) were placed on the sides of the transducer in soft contact with the skin region. Both mini-shakers were excited using a harmonic signal created using a signal wave generator (model AFG3252, Tektronix, Inc., Oregon, United States) and amplified by a power amplifier (type 2718, Brüel and Kjær). The HF-US scanner was operated in power Doppler mode to detect the motion produced and track the mechanical wave propagation. Data were obtained at vibration frequencies f of 200, 300, and 400 Hz, satisfying Nyquist's criterion.

The IQ signals from the HF-US system were processed in MATLAB® 2021a (The Mathworks Inc., Natick, Massachusetts, USA). The Kasai algorithm [20], which allows obtaining the amplitude of the displacements from the variance of the ultrasonic power spectra, was used to produce the crawling wave interference patterns. The crawling waves were pre-processed using DC subtraction and median filter denoising. The estimation of $c_{sw}(\omega)$ was performed with the phase derivative algorithm [17], calculating the phase of the Fourier transform for each point at a specific lateral and axial distance. A flowchart of all stages is presented in Fig. 2. The imaging region of interest (ROI) consisted of a cross-sectional rectangle of 2 mm and 23 mm along the axial and lateral axis. Finally, the average of $c_s(\omega)$ within the ROI at each frequency per volunteer was fit to (8) to estimate the viscoelastic parameters μ_1 and μ_2. A Mann-Whitney U test was performed using MATLAB to test if significant differences in μ_1 and μ_2 values between thigh and forearm locations existed ($P < 0.05$).

III. RESULTS

Doppler motion frames representing crawling wave propagation for vibration frequencies of 200, 300, and 400 Hz are overlapped with B-mode structural images of the anterior thigh skin region of one volunteer in Fig. 3 (A–C), respectively. The estimated shear wave speed maps for each frequency case are shown in Fig. 3 (D–F).

Frequency-dependent shear wave speed plots of each volunteer skin region were fit to the Voigt speed dispersion model (5) as shown in Fig. 4 for both anatomic sites, together with the average of all fitting curves. Overall, the estimated μ_1 and μ_2 were found to be in the range of [1.6 – 6.6] kPa and [2.0 – 4.6] Pa·s, respectively, for the thigh dermis (n = 12 volunteers). For the forearm case, μ_1 and μ_2 was [2.2 - 9.7] kPa and [2.6 - 8.1] Pa·s, respectively (n = 6 volunteers). The average estimated parameters for all volunteers in each skin region are summarized in Table 1 and compared to previous study results in the literature.

IV. DISCUSSION

This study aimed to estimate viscoelastic properties of *in vivo* human healthy dermis using ultrasonic crawling wave elastography based on a HF-US system and a Voigt rheological
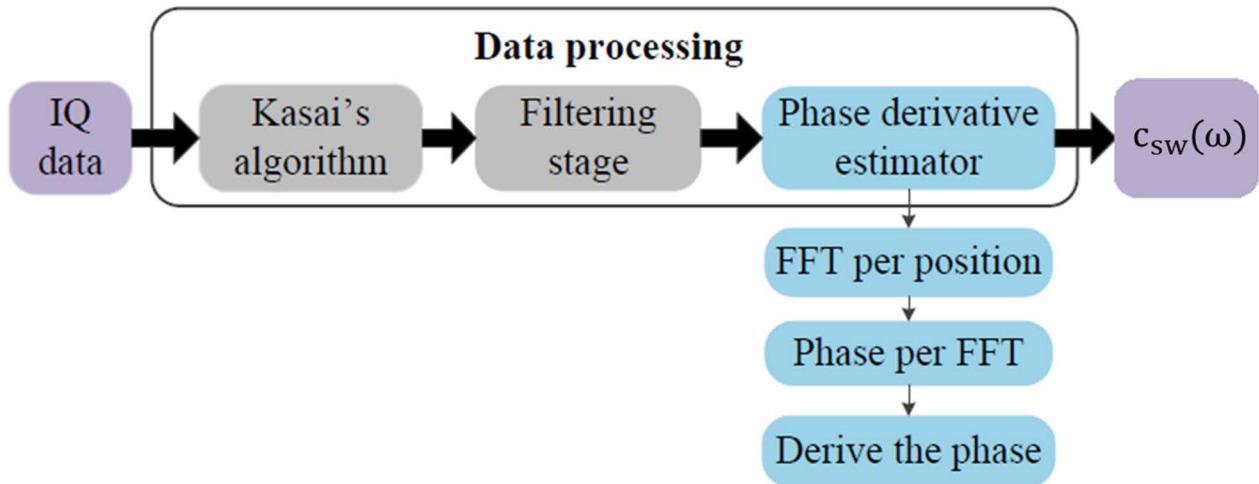
FIGURE 2. Flowchart of the data processing stage $c_{SW}(\omega)$ estimation.

TABLE 1. *In vivo* healthy skin elastography results comparison with previous work.

| Reference	Location	Method [a]	Frequency range (Hz)	Elasticity (kPa)	Shear elasticity [b] (kPa)	Shear viscosity [c] (Pa·s)
This study	Forearm	CrW HF-US	[200,400]	[33.43, 68.18]	6.01±3.12	5.48±1.95
(Liang and Boppart, 2010)	Forearm	Dynamic OCE	[100,600]	[47.2, 121.0]	14.2	6.8
(Zhang *et al.*, 2011)	Forearm	Laser vibrometer	[100,400]	[35.17, 73.26]	10.65±5.67	6.28±5.97
(Zhang *et al.*, 2018)	Forearm	USWE	[100,200]	[11.1, 26.3]	1.67	5.75
This study	Thigh	CrW HF-US	[200,400]	[18.41, 43.20]	3.40±1.82	3.25±0.81
(Zhang *et al.*, 2011)	Thigh	Laser vibrometer	[100,400]	[34.5, 90.6]	9.72±6.24	7.78±11.75

[a] CrW: Crawling wave, HF-US: high-frequency ultrasound, OCE: optical coherence elastography, USWE: ultrasound surface wave elastography.
[b] Shear modulus, and [c] shear viscosity corresponding to this study are reported as mean ± SD (n = 6 for forearm, and n = 12 for thigh).

model of the skin. Few literature reports have evaluated dermis viscoelasticity using ultrasound-based techniques. Liang and Boppart [21] measured Young's modulus of the volar forearm, dorsal forearm, and palm using the dynamic optical coherence elastography technique. They reported a dependence between vibration frequency and wave speed with a mean Young's modulus varying from ~47 kPa to ~121 kPa between 100-600 Hz (i.e., $\mu_1 = 14.2$ kPa and $\mu_2 = 6.8$ Pa·s assuming isotropic and incompressible tissue). Zhang *et al.* [13] used ultrasound surface wave elastography for measuring the SWS of the upper arm and forearm. Forearm SWS was in the range of 2.35 – 3.4 m/s with a frequency-dependent trend (100-200 Hz), corresponding

to $\mu_1 = 1.67$ kPa and $\mu_2 = 5.75$ Pa·s. In addition, Zhang *et al.* [12] evaluated the viscoelastic properties of the thigh and forearm, reporting to $\mu_1 = 9.72 \pm 6.24$ kPa and to $\mu_2 = 7.78 \pm 11.75$ kPa, to $\mu_1 = 10.65 \pm 5.67$ kPa and to $\mu_2 = 6.28 \pm 5.97$ kPa, respectively. Fig. 5 compares the results from this study with the literature in terms of frequency-dependent Young's modulus using (3) and $E \approx 3\mu^2$ (assuming incompressibility of skin).

The appropriateness of the Voigt viscoelastic model in skin tissues was studied before by Kearney *et al.*, [22]. Even though other models such as fractional Voigt and standard-linear-solid (both being a three-parameter model) showed a better fit to the dynamic response in the skin than the
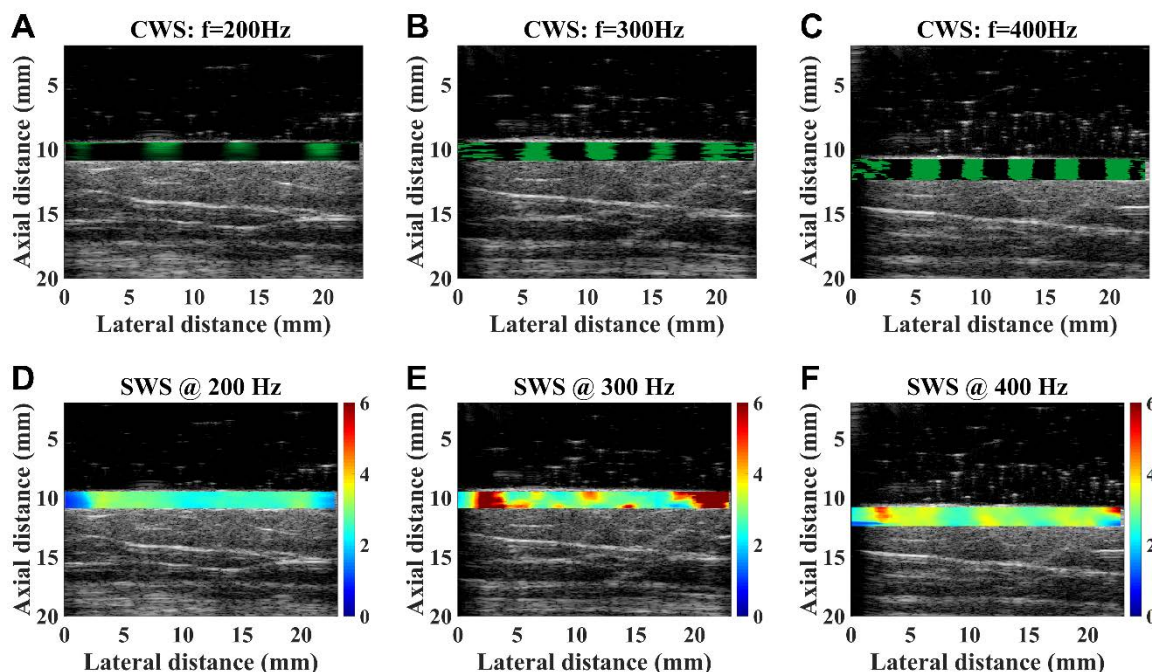
FIGURE 3. B-mode structural images of the anterior thigh skin region of one volunteer superimposed with the Doppler motion frames of crawling waves at vibration frequencies of (A) 200 Hz, (B) 300 Hz, and (C) 400 Hz. Estimated shear wave speed maps (color bar in m/s) of the same skin region are shown in the dermis layer for excitation frequencies of (D) 200 Hz, (E) 300 Hz, and (F) 400 Hz.
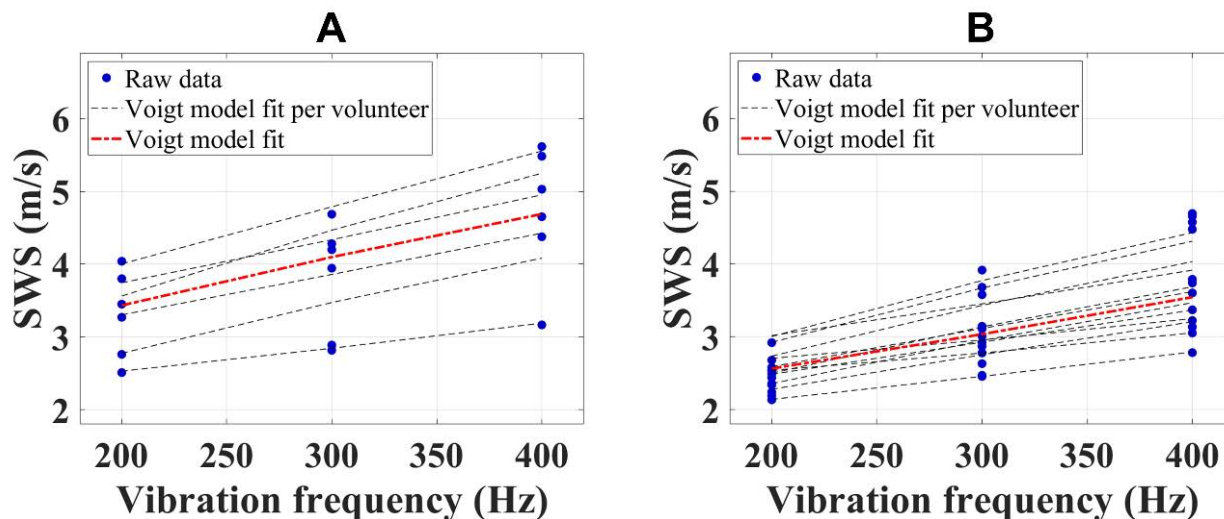

FIGURE 4. Viscoelastic characterization of skin elasticity using the Voigt speed dispersion model (Eq. 8) in frequency-dependent speed plots extracted from (A) forearm dermis ($\mu_1 = 6.01 \pm 3.12$ kPa and $\mu_2 = 5.48 \pm 1.95$ Pa·s, n = 6 volunteers), and (B) thigh dermis with ($\mu_1 = 3.40 \pm 1.82$ kPa and $\mu_2 = 3.25 \pm 0.81$ Pa·s, n = 12 volunteers). The blue dots represent estimations of shear wave speed per frequency and volunteer. Black dashed lines represent individual fitting of Eq. 8 per volunteer. The red line corresponds to the median of all the fitting curves.

Voigt model, the latter only need two parameters (μ_1 and μ_2). Therefore, to avoid overfitting, we decided to use the Voigt model to fit a speed-frequency plot with only three entries (Fig. 4). Moreover, the crawling wave patterns were obtained using only vibrational frequencies up to 400 Hz due to viscous losses, which represented a limiting condition during the experiments.

Overall, in this study, we observed a significantly higher shear elasticity ($P = 0.04$) and shear viscosity ($P = 0.003$)

modulus in the forearm compared to the thigh region. These results are in agreement with *in vivo* results from the skin of young volunteers (25.8 ± 3 years old) using a suction-base commercial cutometer reporting higher immediate elastic distension (i.e., lower stiffness) in the thigh region compared to the dorsal forearm and higher ratio of total retraction to the initial distension (i.e., lower shear viscosity) in the thigh region compared to dorsal forearm [4]. Discrepancies between our results to other wave-based elastography
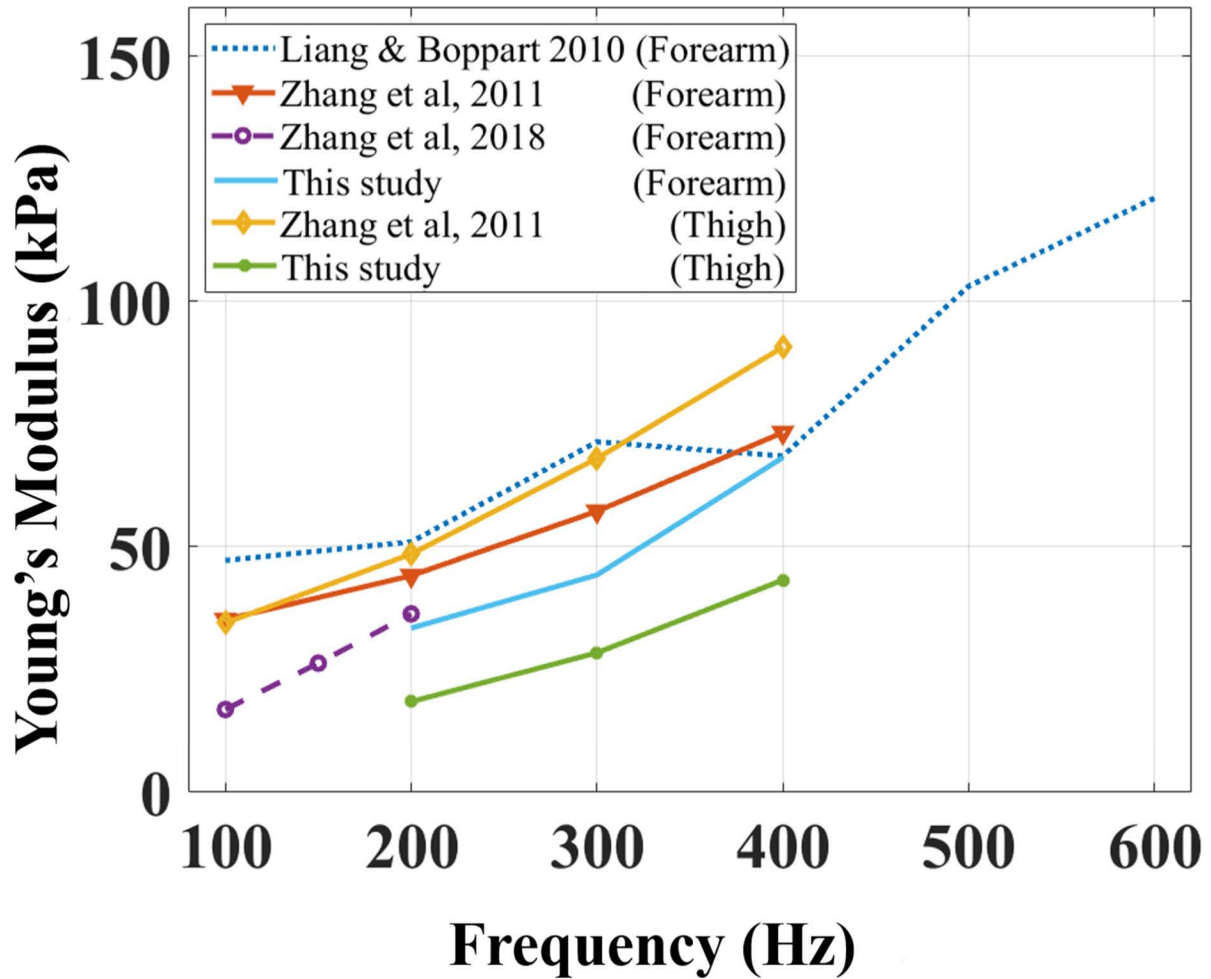
FIGURE 5. Frequency-dependent Young's modulus plot comparison of results from this study and previous literature reports in in vivo skin forearm and thigh regions.

results (inverse behavior found in [12]) may be attributed to variables not considered in this study, including but not limited to ethnic differences, age range, or even hydration conditions. Melanin, responsible for skin pigmentation, plays a crucial role in protecting and preventing sun damage [1], [2]. Some ethnic groups are less prone to be affected by solar irradiation since they possess higher melanin content in their skin. These skin composition differences are believed to explain differences in skin elasticity values with racial differences. Our volunteers correspond to the Hispanic group. No details regarding this issue were reported in the works of Zhang *et al.* [13] and Liang and Boppart [21].

Age can also be a variable that determines the mechanical properties of the skin. Previous studies [23], [24] reported a linear increase in Young's modulus of skin with age, with a simultaneous increasing standard deviation. A linear least-squares model was used to correlate speed (y) and age (x) according to $y = 11.4 + 0.245x$. The mean age of the healthy participants studied by [13] was 45.43 years, whereas Liang and Boppart [20] did not provide details about their cohort of patients. The mean age of the volunteers involved

in our study was 24.5 years. By introducing the mean ages into the relation formulated by Davis *et al.* [24] and dividing them, we obtain a ratio of 1.29; the ratio between the speed obtained by [13] and ours at 200 Hz is 1.21. In that sense, the analysis suggests that age may influence elastic modulus measurement. In addition, hydration – a variable and individual state - was found to influence the elasticity measurements. Hydrated skin exhibited smaller Young's modulus at low vibration frequencies but larger values at higher frequencies, even than those of normal skin [21].

Wave propagation in layered media, such as skin, can be affected not only by the viscoelastic properties of each layer (e.g., complex shear modulus) but also by the thickness of each layer and the properties of the materials connecting its boundaries. Previous work on *in vivo* skin has demonstrated that skin thickness does not have a statistically significant effect on wave speed [25]. In this work, we did not use the full skin model due to its high complexity that requires other unknown variables such as mechanical properties of subsequent layers that are not available during our experiments. In addition, the signal-to-noise ratio of the Doppler

signal was not enough to describe wave propagation at lower layers of the skin. Future work may focus on using an inverse finite element model of the skin, including these cofounding variables, for more realistic viscoelastic characterization of human dermis and other layers.

Additionally, the crawling wave technique was proven to generate accurate shear wave speed dispersion plots by Ormachea *et al.* [26] using tissue-mimicking phantoms and comparing them with mechanical measurements. Future work will evaluate viscoelastic differences between healthy and pathological skin conditions that will inspire the development of biomarkers with clinical relevance.

V. CONCLUSION

In this work, an implementation of crawling waves using a high-frequency ultrasound (HF-US) scanner to estimate the viscoelastic properties of dermal *in vivo* human skin was presented. Results from 18 healthy volunteers show that the shear elasticity and the shear viscosity are higher in the forearm compared to the dorsal forearm locations. The comparison between the obtained results and the literature reports was extensively discussed. Further studies are required to understand the discrepancies between literature reports, as well as to establish an invariable guideline for evaluating the viscoelastic properties of human skin.

ACKNOWLEDGMENT

REFERENCES

[1] E. Berardesca, J. de Rigal, J. L. Leveque, and H. I. Maibach, "*In vivo* biophysical characterization of skin physiological differences in races," *Dermatology*, vol. 182, no. 2, pp. 89–93, 1991.

[2] N. O. Wesley and H. I. Maibach, "Racial (ethnic) differences in skin properties," *Amer. J. Clin. Dermatol.*, vol. 4, no. 12, pp. 843–860, 2003.

[3] C. Liu, S. Assassi, S. Theodore, C. Smith, A. Schill, M. Singh, S. Aglyamov, C. Mohan, and K. V. Larin, "Translational optical coherence elastography for assessment of systemic sclerosis," *J. Biophotonics*, vol. 12, no. 12, Dec. 2019, Art. no. e201900236.

[4] A. B. Cua, K.-P. Wilhelm, and H. I. Maibach, "Elastic properties of human skin: Relation to age, sex, and anatomical region," *Arch. Dermatol. Res.*, vol. 282, no. 5, pp. 283–288, Aug. 1990.

[5] L. Bartolini, F. Feroldi, M. Slaman, J. J. A. Weda, J. F. de Boer, P. van Zuijlen, and D. Iannuzzi, "Toward clinical elastography of dermal tissues: A medical device to probe skin's elasticity through suction, with subsurface imaging via optical coherence tomography," *Rev. Sci. Instrum.*, vol. 91, no. 7, Jul. 2020, Art. no. 074101.

[6] C. Escoffier, J. de Rigal, A. Rochefort, R. Vasselet, J.-L. Lévêque, and P. G. Agache, "Age-related mechanical properties of human skin: An *in vivo* study," *J. Investigative Dermatol.*, vol. 93, no. 3, pp. 353–357, Sep. 1989.

[7] H. Oxlund, J. Manschot, and A. Viidik, "The role of elastin in the mechanical properties of skin," *J. Biomech.*, vol. 21, no. 3, pp. 213–218, Jan. 1988.

[8] C.-C. Luo, L.-X. Qian, G.-Y. Li, Y. Jiang, S. Liang, and Y. Cao, "Determining the *in vivo* elastic properties of dermis layer of human skin using the supersonic shear imaging technique and inverse analysis," *Med. Phys.*, vol. 42, no. 7, pp. 4106–4115, Jun. 2015.

[9] X. Xiang, F. Yan, Y. Yang, Y. Tang, L. Wang, J. Zeng, and L. Qiu, "Quantitative assessment of healthy skin elasticity: Reliability and feasibility of shear wave elastography," *Ultrasound Med. Biol.*, vol. 43, no. 2, pp. 445–452, Feb. 2017.

[10] S. Y. Lee, A. R. Cardones, J. Doherty, K. Nightingale, and M. Palmeri, "Preliminary results on the feasibility of using ARFI/SWEI to assess cutaneous sclerotic diseases," *Ultrasound Med. Biol.*, vol. 41, no. 11, pp. 2806–2819, Nov. 2015.

[11] A. C. Saavedra, J. Arroyo, F. Zvietcovich, R. J. Lavarello, and B. Castaneda, "*In vivo* estimation of the Young's modulus in normal human dermis," in *Proc. 40th Annu. Int. Conf. IEEE Eng. Med. Biol. Soc. (EMBC)*, Jul. 2018, pp. 3456–3459.

[12] X. Zhang, T. G. Osborn, M. R. Pittelkow, B. Qiang, R. R. Kinnick, and J. F. Greenleaf, "Quantitative assessment of scleroderma by surface wave technique," *Med. Eng. Phys.*, vol. 33, no. 1, pp. 31–37, 2011.

[13] X. Zhang, B. Zhou, S. Kalra, B. Bartholmai, J. F. Greenleaf, and T. Osborn, "An ultrasound surface wave technique for assessing skin and lung diseases," *Ultrasound Med. Boil.*, vol. 44, no. 2, pp. 321–331, 2018.

[14] Z. Wu, L. S. Taylor, D. J. Rubens, and K. J. Parker, "Sonoelastographic imaging of interference patterns for estimation of the shear velocity of homogeneous biomaterials," *Phys. Med. Biol.*, vol. 49, no. 6, pp. 911–922, Feb. 2004.

[15] K. F. Graff, *Wave Motion in Elastic Solids*. New York, NY, USA: Dover, 1991.

[16] A. C. Saavedra, F. Zvietcovich, R. J. Lavarello, and B. Castaneda, "Measurement of surface acoustic waves in high-frequency ultrasound: Preliminary results," in *Proc. 39th Annu. Int. Conf. IEEE Eng. Med. Biol. Soc. (EMBC)*, Jul. 2017, pp. 3000–3003.

[17] Z. Hah, C. Hazard, B. Mills, C. Barry, D. Rubens, and K. Parker, "Integration of crawling waves in an ultrasound imaging system. Part 2: Signal processing and applications," *Ultrasound Med. Biol.*, vol. 38, no. 2, pp. 312–323, 2012.

[18] F. H. Silver, J. W. Freeman, and D. DeVore, "Viscoelastic properties of human skin and processed dermis," *Skin Res. Technol.*, vol. 7, no. 1, pp. 18–23, Feb. 2001.

[19] E. L. Carstensen and K. J. Parker, "Physical models of tissue in shear Fields," *Ultrasound Med. Biol.*, vol. 40, no. 4, pp. 655–674, 2014.

[20] C. Kasai, K. Namekawa, A. Koyano, and R. Omoto, "Real-time two-dimensional blood flow imaging using an autocorrelation technique," *IEEE Trans. Sonics Ultrason.*, vol. SU-32, no. 3, pp. 458–464, May 1985.

[21] X. Liang and S. A. Boppart, "Biomechanical properties of *in vivo* human skin from dynamic optical coherence elastography," *IEEE Trans. Biomed. Eng.*, vol. 57, no. 4, pp. 953–959, Apr. 2010.

[22] S. P. Kearney, A. Khan, Z. Dai, and T. J. Royston, "Dynamic viscoelastic models of human skin using optical elastography," *Phys. Med. Biol.*, vol. 60, no. 17, pp. 6975–6990, Sep. 2015.

[23] R. Grahame and P. J. Holt, "The influence of ageing on the *in vivo* elasticity of human skin," *Gerontologia*, vol. 15, no. 2, pp. 39–121, 1969.

[24] B. R. Davis, E. Bahniuk, J. K. Young, C. M. Barnard, and J. M. Mansour, "Age-dependent changes in the shear wave propagation through human skin," *Experim. Gerontol.*, vol. 24, no. 3, pp. 201–210, 1989.

[25] A. E. Knight, A. B. Pely, F. Q. Jin, A. R. Cardones, M. L. Palmeri, and K. R. Nightingale, "Analysis of factors affecting shear wave speed in *in vivo* skin," in *Proc. IEEE Int. Ultrason. Symp. (IUS)*, Oct. 2019, pp. 970–973.

[26] J. Ormachea, R. J. Lavarello, S. A. McAleavey, K. J. Parker, and B. Castaneda, "Shear wave speed measurements using crawling wave sonoelastography and single tracking location shear wave elasticity imaging for tissue characterization," *IEEE Trans. Ultrason., Ferroelect., Freq. Control*, vol. 63, no. 9, pp. 1351–1360, Sep. 2016.

ANA C. SAAVEDRA (Member, IEEE) received the B.S. degree in electronics engineering and the M.S. degree in digital signal and image processing from the Pontificia Universidad Católica del Perú, Lima, Peru, in 2015 and 2018, respectively. She is currently pursuing the Ph.D. degree in biomedical engineering with the University of Michigan, Ann Arbor, MI, USA. Her current research interests include medical imaging, ultrasound elastography, tissue characterization, and convolutional neural networks.

JUNIOR ARROYO received the B.S. degree in physics and the M.S. degree in digital signal and image processing from the Pontificia Universidad Católica del Perú, Lima, Peru, in 2014 and 2017, respectively. He is currently pursuing the Ph.D. degree in biomedical engineering with Johns Hopkins University, Baltimore, MD, USA. His research interests include ultrasound, elastography, biomaterials, and photoacoustics.

GILMER FLORES (Member, IEEE) received the B.S. degree in electrical engineering from the Pontificia Universidad Católica del Perú, Lima, Peru, in 2020.

He is currently the Laboratory Assistant with the Medical Imaging Laboratory, Pontificia Universidad Católica del Perú. His current research interests include medical imaging, ultrasound elastography, and tissue characterization.

FERNANDO ZVIETCOVICH received the B.S. degree in electrical engineering and the M.S. degree in digital signal and image processing from the Pontificia Universidad Catholica del Perú, Lima, Peru, in 2012 and 2014, respectively, and the Ph.D. degree in electrical engineering from the University of Rochester, Rochester, NY, USA, in 2020. He is currently working with the Biomedical Optics Laboratory, Department of Biomedical Engineering, University of Houston, Houston, TX, USA. He is also working as a Research Fellow with the Institute of Optics, Spanish National Research Council (CSIC), Madrid, Spain. His current research interests include novel wave-based optical coherence elastography methods in soft tissues for advancing the diagnosis and monitoring of diseases and treatments in clinical environments, optical coherence tomography, medical elastography, medical image formation and processing, and computer vision and pattern recognition applied to medicine. He is the Holder of the 2020 SPIE-Franz Hillenkamp Postdoctoral Fellowship in Problem-Driven Biomedical Optics and Analytics.

BENJAMIN CASTANEDA (Senior Member, IEEE) received the M.Sc. degree in computer engineering from the Rochester Institute of Technology, NY, USA, and the Ph.D. degree in electrical engineering from the University of Rochester, NY, USA.

After his Ph.D. degree, he founded the Medical Imaging Laboratory, Pontificia Universidad Católica del Perú (PUCP), where he is currently a Full Professor in electrical engineering and the Director of Research and Innovation with the Department of Engineering.

He has more than 15 years of experience on biomedical ultrasound and medical imaging analysis. His research interests include quantitative elastographic imaging (breast cancer diagnosis, prostate cancer detection, and skin characterization), computed aided diagnosis tools (automated diagnosis of Tuberculosis, spondyloarthrosis, follow-up of treatment for Leishmaniasis, and preventive diagnosis in maternal-perinatal health), and telemedicine (obstetric ultrasound and colposcopy).

Dr. Castaneda has been twice finalist for the Young Investigator Award from the American Institute of Ultrasound in Medicine, in 2007 and 2011, for his research work. He received an honorable mention from the worldwide engineering contest of Mondialogo (sponsored by UNESCO and Daimler, in 2007), and an honorable mention in the SPIE Medical Imaging International Conference, in 2008. In 2013, he received the Academic Innovator Award from the Peruvian Government for his continuous work in the development of medical technology (SINACYT/CONCYTEC, in 2013). The same year, he won the Best Patent from the Peruvian Government (INDECOPI, in 2013) for an automated staining system for tuberculosis detection. The same invention received a silver medal at the International Exhibition of Inventions of Geneva, in 2014. He is also the Founder of Medical Innovation & Technology, a Peruvian start-up focused on the development of telemedicine technology for rural areas. He is currently a member of the Peruvian Committee for Health Informatics and an Associate Member of the IEEE Bio Imaging and Signal Processing Technical Committee.

ROBERTO J. LAVARELLO (Senior Member, IEEE) received the B.Sc. degree in electronics engineering from the Pontificia Universidad Católica del Perú, in 2000, and the M.Sc. and Ph.D. degrees in electrical and computer engineering from the University of Illinois at Urbana–Champaign, in 2005 and 2009, respectively. He is currently a Full Professor with the Department of Engineering, Pontificia Universidad Católica del Perú, and the Director of the Medical Imaging Laboratory. His research interests include reconstruction and processing of images for the non-invasive assessment of pathological conditions. He is a Former Fulbright Scholarship Recipient. He is a member of the IEEE EMBS Technical Committee on Biomedical Imaging and Image Processing, the IEEE SPS Technical Committee on Bio Imaging and Signal Processing, and the Technical Program Committee of the IEEE International Ultrasonics Symposium. He served as an Associate Editor for the IEEE Transactions on Biomedical Engineering (2010–2012). He is currently an Associate Editor of the IEEE Transactions on Ultrasonics, Ferroelectrics and Frequency Control and the IEEE Transactions on Medical Imaging, and an Editorial Board Member of the IEEE Open Access Journal of Engineering in Medicine and Biology. He has served as an IEEE EMBS Peru Section Chapter Chair (2014–2016). He is currently the R9 Representative at the IEEE EMBS AdCom (2017–2022), the Chair of the IEEE Transactions on Medical Imaging Steering Committee, the Chair of the IEEE International Symposium on Biomedical Imaging Steering Committee, and the Co-Chair of the Backscatter Coefficient Group, AIUM/QIBA Pulse-Echo Quantitative Ultrasound Biomarker Committee.

● ● ●